THE JOURNAL OF BIOLOGICAL CHEMISTRY VOL. 290, NO. 47, pp. 28156–28165, November 20, 2015

The Regulatory and Kinase Domains but Not the Interdomain Linker Determine Human Double-stranded RNA-activated Kinase (PKR) Sensitivity to Inhibition by Viral Non-coding RNAs*

Received for publication, July 27, 2015, and in revised form, September 24, 2015 Published, JBC Papers in Press, October 2, 2015, DOI 10.1074/jbc.M115.679738

S. Sunita[1], **Samantha L. Schwartz**[1], **and Graeme L. Conn**[2]

From the Department of Biochemistry, Emory University School of Medicine, Atlanta, Georgia 30322

Background: Human PKR (hPKR) interdomain linker (IDL), regulatory domain, and kinase domain contributions to RNA-mediated regulation are incompletely defined.
Results: Whereas the IDL plays no role, both domains are involved in RNA-mediated inhibition.
Conclusion: hPKR susceptibility to viral RNA inhibitors is dictated by determinants in both domains.
Significance: Human viruses evolved non-coding RNA features specific to potent hPKR inhibition.

Double-stranded RNA (dsRNA)-activated protein kinase (PKR) is an important component of the innate immune system that presents a crucial first line of defense against viral infection. PKR has a modular architecture comprising a regulatory N-terminal dsRNA binding domain and a C-terminal kinase domain interposed by an unstructured ~80-residue interdomain linker (IDL). Guided by sequence alignment, we created IDL deletions in human PKR (hPKR) and regulatory/kinase domain swap human-rat chimeric PKRs to assess the contributions of each domain and the IDL to regulation of the kinase activity by RNA. Using circular dichroism spectroscopy, limited proteolysis, kinase assays, and isothermal titration calorimetry, we show that each PKR protein is properly folded with similar domain boundaries and that each exhibits comparable polyinosinic-cytidylic (poly(rI:rC)) dsRNA activation profiles and binding affinities for adenoviral virus-associated RNA I (VA RNA_I) and HIV-1 *trans*-activation response (TAR) RNA. From these results we conclude that the IDL of PKR is not required for RNA binding or mediating changes in protein conformation or domain interactions necessary for PKR regulation by RNA. In contrast, inhibition of rat PKR by VA RNA_I and TAR RNA was found to be weaker than for hPKR by 7- and >300-fold, respectively, and each human-rat chimeric domain-swapped protein showed intermediate levels of inhibition. These findings indicate that PKR sequence or structural elements in the kinase domain, present in hPKR but absent in rat PKR, are exploited by viral non-coding RNAs to accomplish efficient inhibition of PKR.

Phosphorylation of the eukaryotic translation initiation factor eIF2 is a critical regulatory mechanism for control of eukaryotic protein synthesis. Four mammalian kinases act on eIF2α in response to different stress stimuli: double-stranded RNA (dsRNA)[3]-activated protein kinase (PKR), heme-regulated inhibitor kinase, PKR-like endoplasmic reticulum kinase, and general control nonderepressible 2 (1). Among these, PKR plays a crucial role in the innate immune system's primary response to cellular viral infection.

PKR has a modular architecture composed of an N-terminal regulatory dsRNA binding domain (dsRBD; residues 1–169 in human PKR) containing two tandem N-terminal dsRNA binding motifs (dsRBM 1 and 2) and a C-terminal kinase domain (KD; residues 252–551). These structured domains are separated by an 82-residue interdomain linker (IDL) region (Fig. 1*A*). The dsRBD additionally has an ~22-amino acid unstructured linker between the two dsRBMs that is proposed to wrap around the dsRNA to allow optimal interaction of each dsRBM with the A-form RNA helix (2). The KD fold possesses two lobes connected by a small hinge region, with distinct functional roles: the smaller N-terminal lobe mediates PKR dimerization, whereas the larger C-terminal lobe interacts with the eIF2α substrate (3). The IDL separating the regulatory domain from the catalytic domain is unstructured in solution but has been speculated to play a role in mediating communication between the two structured domains during activation by dsRNA (4, 5).

How the kinase activity of PKR is controlled in the absence of activating RNA has been the subject of debate. An autoinhibition model for PKR activation was originally proposed in which direct interaction of the N-terminal dsRBD and KD inhibits the latent kinase activity before the dsRNA-mediated release of this inhibition (6, 7). However, several lines of evidence argued for

* This work was supported in part by National Institute of Allergy and Infectious Diseases, National Institutes of Health Grant R21-AI097803 and a grant from the Emory University Research Council (URC 2010050). The authors declare that they have no conflicts of interest with the contents of this article.
[1] Both authors contributed equally and should be considered joint first authors.
[2] To whom correspondence should be addressed: Dept. of Biochemistry, Emory University School of Medicine, 1510 Clifton Rd. NE, Atlanta GA 30322. Tel.: 404-727-5965; Fax: 404-727-2738; E-mail: gconn@emory.edu.

[3] The abbreviations used are: dsRNA, double-stranded RNA; Ad2, adenovirus type 2; CTD, C-terminal domain; dsRBD, double-stranded RNA binding domain; dsRBM, double-stranded RNA binding motif; IDL, interdomain linker; KD, kinase domain; NTD, N-terminal domain; PKR, double-stranded RNA-activated protein kinase; rPKR, rat PKR; hPKR, human PKR; TAR, *trans*-activation response (element of HIV-1); VA RNA_I, virus-associated RNA I.

an alternative model in which dsRNA-mediated PKR dimerization is the critical step in activation (8). Latent PKR binds ATP, exists predominantly as an extended monomeric structure, and is capable of forming weak dimers in solution and autophosphorylation in a PKR concentration-dependent manner (>500 nM) in the absence of dsRNA (5, 9–12). Constitutive PKR activation from fusion of heterologous dimerization domains to the isolated PKR KD provides further evidence for the sufficiency of PKR dimerization for kinase activation (13, 14). Finally, the identification of a cellular non-coding RNA inhibitor of latent PKR, the loss of which is implicated in various cancers (15, 16), suggests a necessity for exogenous control of PKR kinase activity.

The best characterized role of PKR is as a sensor of cytosolic dsRNA. dsRNA represents a potent pathogen-associated molecular pattern, present in some viral genomes or produced as a consequence of viral gene expression and replication (17). Viral dsRNA-promoted PKR homodimerization leads to subsequent autophosphorylation and kinase activation (8, 18). Activated PKR phosphorylates Ser-51 of the α subunit of eIF2, converting eIF2 into an inhibitor of its guanine exchange factor, eIF2B (1). eIF2 is thus sequestered in an inactive form, blocking initiation of cellular protein translation. Diverse viruses have evolved varied strategies to circumvent this PKR-mediated blockade of translation (19), including expression of "RNA decoys" that bind but do not activate PKR. The best characterized of these viral RNA inhibitors of PKR is the essential proviral non-coding "virus-associated" RNA (VA RNA) present in at least one copy in the genome of all human adenoviruses (20–22). Other viral non-coding RNAs capable of inhibiting PKR include EBER-1 of Epstein-Barr virus (23, 24), and the HIV-1 *trans*-activation response (TAR) RNA element present both in viral mRNAs and as a short transcript of ~60 nucleotides (25). Although the model for PKR activation via dimerization on dsRNA is well established (8), the precise mechanism of action of these viral RNA inhibitors is less clear. Recent evidence from small angle x-ray scattering studies suggests that the structure of VA RNA_I is precisely tuned to present a single high affinity PKR binding site (26). However, whether such viral RNAs function by binding PKR exclusively via its N-terminal dsRNA domain (dsRBDs) to block PKR dimerization, or additionally require regions within the C-terminal KD or the IDL, is not known.

Here, we present the design and analysis of PKR IDL deletion and human-rat PKR domain swap variants to address the potential role(s) of the IDL and each PKR domain to RNA-mediated regulation. Our results show that complete deletion of the human PKR (hPKR) IDL has no effect on the activation or inhibition of kinase activity by RNA. In contrast, we find that both the N-terminal dsRBD and the C-terminal KD of hPKR are required for inhibition by human viral non-coding RNAs.

Experimental Procedures

Cloning of Human PKR (hPKR) Variants—IDL deletion variants of hPKR within the pET-hPKR/PPase (10) were created by MEGAWHOP mutagenesis (27, 28) based on sequence alignment with murine homologs (mouse, rat, and hamster). Three hPKR IDL deletions were created (Fig. 1, *A* and *B*): IDLΔ1 (ΔT197-T212), IDLΔ2 (ΔT170-L227), and IDLΔ3 (ΔT170-D251). The alignment also identified a region in the human PKR KD that is absent in the other homologs and previously deleted in the human PKR KD construct used to determine its crystal structure in complex with eIF2α (3). This kinase deletion (ΔD338-N350; Fig. 1*A*) was additionally included in some of the constructs generated in this study (those denoted with *asterisks*). Other than hPKR-IDLΔ1 and hPKR-IDLΔ1*, the hPKR IDL deletion variants required the use of an N-terminal SUMO tag (obtained by PCR amplification of the Smt3 sequence from the pE-SUMO plasmid vector; denoted *S*) for optimal expression and solubility. S-hPKR-IDLΔ2, S-hPKR-IDLΔ2*, and S-hPKR-IDLΔ3* in the pET/PPase background were generated by overlap extension PCR to add the N-terminal His_6-SUMO tag and MEGAWHOP mutagenesis to generate the deletions.

DNA encoding rat PKR (rPKR) with codon optimization for expression in *Escherichia coli* was obtained from Genscript and subcloned into the pET/PPase plasmid with an N-terminal His_6-SUMO tag after digestion with KpnI and BamHI to create an S-rPKR expression construct. Human-rat chimeric PKR expression plasmids were created based on alignment of hPKR with the mouse and rat sequences. The region spanning Thr-170 to Ser-192 of hPKR was taken as the "breakpoint" for domain switching in order to generate S-r/hPKR (rat dsRBD and human KD) and S-h/rPKR (human dsRBD and rat KD).

Protein Expression and Purification—E. coli Rosetta2(DE3) cells were transformed with each PKR-encoding plasmid and plated on LB-agar containing ampicillin (100 μg/ml) and chloramphenicol (34 μg/ml). For PKR constructs without an N-terminal His_6-SUMO tag, soluble protein expression was accomplished using overnight autoinduction (29) at 20 °C after initial growth at 37 °C for 6 h. For N-terminal His_6-SUMO-tagged proteins, cells were grown in Terrific Broth (TB) at 37 °C and induced at mid-log phase using isopropyl 1-thio-β-D-galactopyranoside (0.1 mM), and growth continued overnight at 20 °C for protein expression.

Tagless PKR proteins were purified using three sequential chromatographic steps performed on an ÄKTApurifier10 FPLC system: heparin affinity (HiPrep Heparin 16/10), poly(rI:rC) dsRNA-affinity (30) and gel filtration (Superdex 200 10/300). Each step was performed with the column pre-equilibrated in 20 mM HEPES buffer (pH 7–8.5; adjusted to at least one unit above the predicted protein pI) containing 150 mM NaCl, 10% (v/v) glycerol, 0.1 mM EDTA, and 10 mM β-mercaptoethanol, except that EDTA was omitted for the final gel filtration column. Proteins were eluted from the heparin-affinity column using a linear gradient of NaCl from 0.15 to 1.5 M over five column volumes. Pooled protein fractions were diluted with the same buffer without NaCl to reduce the NaCl concentration to ~150 mM and applied to the poly(rI:rC) dsRNA affinity column. PKR proteins were again eluted using a linear gradient of NaCl from 0.15 to 1.5 M over five column volumes. Pooled PKR-containing fractions were either flash-frozen for storage at −80 °C or applied directly to the gel filtration column and eluted isocratically. PKR-containing fractions from the gel filtration column were pooled, and the protein was used directly in the experiments described.

For N-terminal His_6-SUMO-tagged PKR proteins, Ni^{2+} affinity was used as the first step in place of heparin affinity. The column (HisTrap FF Crude 1 ml) was pre-equilibrated with 20 mM Tris HCl (pH 7–8.5) buffer containing 500 mM NaCl, 20 mM imidazole, and 10 mM β-mercaptoethanol. Bound proteins were eluted using an imidazole gradient (20–400 mM, over 10 column volumes) in the same buffer. PKR-containing fractions were pooled, diluted with salt-free buffer to give a final concentration of ~150 mM NaCl, and further purified using poly (rI:rC) dsRNA affinity and gel filtration chromatographies as described for the tagless proteins.

Where used, cleavage of the N-terminal His_6-SUMO tag was accomplished by buffer exchange into SUMO cleavage buffer (50 mM Tris HCl (pH 7.5), 2 mM DTT, 150 mM NaCl, and 10% glycerol) and treatment of the fusion protein with SUMO protease (Life Sensors) at 4 °C overnight. Cleaved PKR proteins were purified from the free His_6-SUMO tag and uncleaved fusion using a final round of gel filtration chromatography.

RNA in Vitro Transcription and Purification—A truncated form of human adenovirus type 2 (Ad2) VA RNA_I (94 nucleotides), which retains full wild-type activity but lacks the entire terminal stem ("TSΔ21") and a short sequence in the apical stem ("A2dl2") was *in vitro* transcribed using T7 RNA polymerase under previously established optimal conditions (31, 32). HIV-1 TAR RNA (59 nucleotides) was also prepared by T7 RNA polymerase run-off transcription using established conditions (33, 34). Transcripts were resolved by preparative denaturing (50% urea) polyacrylamide gel electrophoresis (PAGE; 10% acrylamide), excised from the gel, and recovered by electroelution using a Biotrap device (Schleicher and Schuell). RNAs were annealed in 1× Tris-EDTA buffer and dialyzed overnight against the appropriate assay buffer before use. To verify the absence of dimerized RNA that would confound interpretation of PKR inhibition assays (35), purified HIV-1 TAR RNA was examined by native PAGE (10% acrylamide) and stained with SYBR Gold.

Kinase Activity Assays Using Slot Blot or SDS-PAGE—Slot blot assays of PKR autophosphorylation contained PKR (0.1 μg) in 50 mM Tris buffer (pH 7.8) with poly(rI:rC) dsRNA (0–100 μg/ml), 20 μM ATP, 1 μCi of [γ-^{32}P]ATP (10 mCi/ml, 6000 Ci/mmol), 50 mM KCl, 2 mM $MgCl_2$, 2.5 mM DTT, and 10% glycerol in a total reaction volume of 10 μl. SDS-PAGE assays of PKR autophosphorylation and eIF2α phosphorylation were performed identically but included eIF2α (0.25 μg) in the absence or presence of a single concentration of poly(rI:rC) dsRNA (0.3 μg/ml). Reactions were incubated at 25 °C for 10 min and then stopped by the addition of gel loading dye (for SDS-PAGE analysis) or 400 μl of ice-cold phosphate-buffered saline containing 200 μM ATP (for slot blot analysis). In the latter case quenched samples were applied promptly to a Bio-Dot SF (Bio-Rad) microfiltration system, and proteins were bound to a nitrocellulose membrane under vacuum. The membrane was washed to remove unreacted [γ-^{32}P]ATP and then air-dried. For both membranes and dried SDS-PAGE gels, the extent of PKR and eIF2α phosphorylation was determined by exposure to a phosphor storage screen and analysis using a Typhoon FLA 7000 PhosphorImager and ImageQuant software (GE Healthcare).

PKR inhibition assays were performed in a similar manner but included a 10-min preincubation step at 25 °C with the *in vitro* transcribed RNA (0–100 μM) and PKR (0.1 μg) in 50 mM Tris buffer (pH 7.8) containing 50 mM KCl, 2.5 mM DTT, and 10% glycerol. Reactions (10 μl final volume) were initiated by the addition of 0.04 μg/ml poly(rI:rC) dsRNA, 20 μM ATP, 1 μCi of [γ-^{32}P]ATP (10 mCi/ml, 6000 Ci/mmol), and 2 mM $MgCl_2$. After a 10-min incubation at 25 °C, the reactions were quenched, and the products were quantified as described above for the activation assays. IC_{50} values were obtained by nonlinear regression analysis using the log(inhibitor) *versus* response equation in GraphPad Prism software.

Circular Dichroism (CD) Spectroscopy—CD spectra (250–190 nm) of protein (5–10 μM) in 10 mM sodium phosphate (pH 7.5) and 10% glycerol were recorded at 25 °C on a Jasco J810 spectrophotometer using a quartz cuvette with a 0.1-cm path length and instrument settings of 1-nm bandwidth, 0.2-nm step size, and 16-s averaging time. Spectra were recorded in triplicate and averaged, and background was subtracted before unit conversion to mean residue ellipticity (36).

Limited Proteolysis—Purified proteins were diluted to a concentration of ~0.2 mg/ml in gel filtration buffer and digested by different ratios of trypsin:PKR (1:10,000, 1:5,000, 1:1,000) at 20 °C for 45 min. The reaction products were resolved by SDS-PAGE (10% acrylamide) and visualized by staining with Coomassie Brilliant Blue.

Isothermal Titration Calorimetry—Binding affinities of VA RNA_I or HIV-1 TAR for select PKR variants were measured using an Auto-iTC_{200} microcalorimeter (Malvern/MicroCal). Samples were prepared by dialyzing overnight against 50 mM Tris buffer (pH 7.5) containing 100 mM NaCl, and the experiments were performed by titrating RNA (80 μM) into the sample cell containing PKR (10–15 μM) at 25 °C in 16 × 2.5-μl injections with 150-s spacing. Titration curves were fit by a non-linear least squares method in MicroCal Origin software using the single site binding model.

Results

Design and Expression of IDL Deletion PKR Variants—hPKR is a 551-amino acid protein with an N-terminal dsRBD (residues 1–169) and C-terminal catalytic domain (KD; residues 252–551) (Fig. 1*A*) separated by a highly acidic and unstructured IDL. To examine the potential role of the hPKR IDL in dsRNA-mediated activation and inhibition of its kinase activity, we used the known hPKR domain boundaries and sequence alignment with PKR homologs from rodent species as a guide to design three IDL deletion variants (Fig. 1, *A* and *B*). Specifically, hPKR-IDLΔ1 and hPKR-IDLΔ2 were designed to mirror the short natural IDL deletion in mouse/rat PKR (mPKR/rPKR) and the larger IDL deletion of variant 2 of the Golden Hamster protein (*Mesocricetus auratus* PKR), respectively. The third construct, hPKR-IDLΔ3 corresponds to complete deletion of the hPKR IDL. These proteins lack a total of 16, 58, and 82 residues from the hPKR IDL, respectively (Fig. 1, *A* and *B*).

Wild-type hPKR and hPKR-IDLΔ1 were expressed and purified using established protocols (10, 30), whereas the shorter IDLΔ2 and IDLΔ3 constructs were insoluble when expressed in *E. coli*. We found that the addition of an N-terminal SUMO

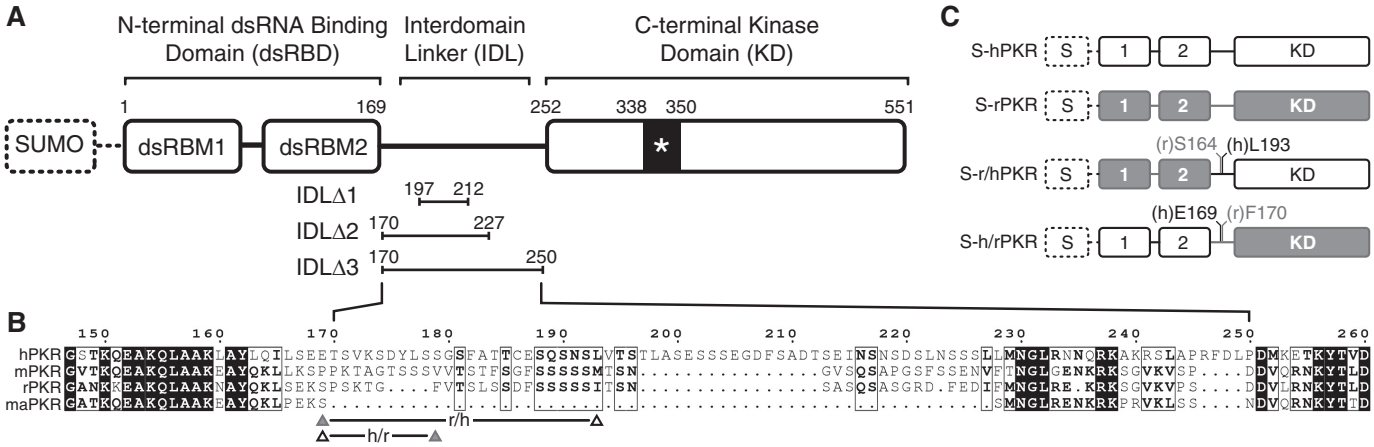

FIGURE 1. **PKR domain organization and design of PKR variants.** *A*, domain architecture and boundaries within hPKR. The locations and boundaries of the N-terminal dsRBD consisting of two dsRNA binding motifs, the IDL, and catalytic KD are indicated. Also noted are the placement of an N-terminal SUMO tag (*dashed line box* and denoted *S* elsewhere) and KD deletion (ΔD338-N350, denoted *) used in some expression constructs (see "Experimental Procedures" for details). Residues removed in each of the IDL deletion constructs are noted below. *B*, alignment of human (*h*), mouse (*m*), rat (*r*), and hamster (*ma*) PKR sequences within the IDL. *C*, design of human-rat NTD/KD domain swap chimeric PKR proteins. The last NTD residue and first KD residue used in each of the chimeric proteins are indicated, and these positions highlighted beneath the sequence alignment of *panel B*.

(smt3) tag allowed soluble expression of both shorter constructs. Importantly, the addition of the SUMO tag had no discernible effect on hPKR activation or inhibition by poly(rI:rC) dsRNA and Ad2 VA RNA_I (30, 32), respectively (Fig. 2, *A* and *B*). Additionally, we tested the effect of a short deletion in the KD (residues 338–350), previously shown to reduce the tendency of PKR to form high molecular weight aggregates at high concentration (3), on the solubility and stability of hPKR proteins with IDL deletions. The PKR constructs with and without the additional KD deletion expressed similarly and had similar profiles of response to activating and inhibitory dsRNAs (Fig. 2, *C* and *D*, and data not shown). Regardless of the presence or absence of an N-terminal SUMO tag or deletions within the IDL or KD, each protein eluted predominantly in a monomeric form from the gel filtration column used as the final step of purification.

IDL Deletions Do Not Change the Structure or Regulation of hPKR by RNA—Wild-type hPKR and each IDL deletion mutant was analyzed by far UV CD spectroscopy (Fig. 3*A*) after removal of the N-terminal SUMO tag for hPKR-IDLΔ2 and hPKR-IDLΔ3*. The spectra revealed that each protein is well folded as suggested by gel filtration chromatography. Furthermore, the spectra were essentially superimposable demonstrating that none of the IDL deletions altered the secondary structure content of the remaining two major domains. The spectra are also consistent with prior observations that the IDL region is flexible and lacks defined α-helical or β-sheet secondary structure.

The first steps in RNA-mediated PKR activation involve PKR dimerization on dsRNA and autophosphorylation. The activation of PKR follows a bell-shaped curve where the extent of activation initially increases with the concentration of dsRNA but then declines at the highest activator concentrations as PKR binds in a monomeric form to different dsRNA molecules (37, 38). Assays of PKR autophosphorylation in the presence of [γ-^{32}P]ATP are established as a direct readout of PKR activation (32) and were used to assess the activation and inhibition of each IDL deletion mutant by poly(rI:rC) dsRNA and VA RNA_I, respectively. In both cases the regulation of PKR by RNA was essentially unaffected by any of the three IDL deletions; PKR activation followed a bell-shaped curve with approximately the same maximum poly(rI:rC) dsRNA concentration, and inhibition by VA RNA_I was accomplished with similar IC_{50} values (Fig. 3, *B* and *C*, and Table 1). We conclude from these results that the IDL deletions do not alter the structural elements responsible for recognizing and responding to activator or inhibitor RNAs, including communication between the N-terminal regulatory domain and C-terminal kinase domain. The hPKR IDL appears to play no role in control of dsRNA-mediated PKR regulation.

PKR Domain Substitutions Do Not Significantly Alter Protein Boundaries or Activation by dsRNA—In the absence of any apparent role for the IDL, we next asked whether each folded domain might influence PKR regulation by different RNAs. For example, whereas binding of dsRNA of sufficient length via the N-terminal regulatory domain might be sufficient to drive activation by promoting PKR dimerization, it is less clear whether RNA-mediated inhibition is exclusively controlled by interaction with the two N-terminal dsRNA binding motifs. To address this question, we speculated that hPKR and rPKR might exhibit differential sensitivity to a human viral inhibitor non-coding RNA that could be exploited to dissect the relative contributions of each folded domain to the process of RNA-mediated inhibition. Thus, we first compared inhibition of hPKR and rPKR by human Ad2 VA RNA_I. Soluble expression and purification of rPKR required the use of an N-terminal SUMO (smt3) fusion. Therefore, although hPKR and S-hPKR were essentially indistinguishable in their responses to poly(rI:rC) dsRNA and VA RNA_I (Fig. 2) the latter human protein was used for this comparison as well as subsequent analyses. Consistent with our anticipation, the human non-coding viral transcript was a significantly weaker inhibitor of rPKR than the human homolog (Fig. 4 and Table 1).

To assess the specific contribution of each PKR domain to this differential sensitivity to VA RNA_I-mediated inhibition, we generated chimeric N- and C-terminal domain swap variants of hPKR and rPKR. Again, each chimeric construct was expressed

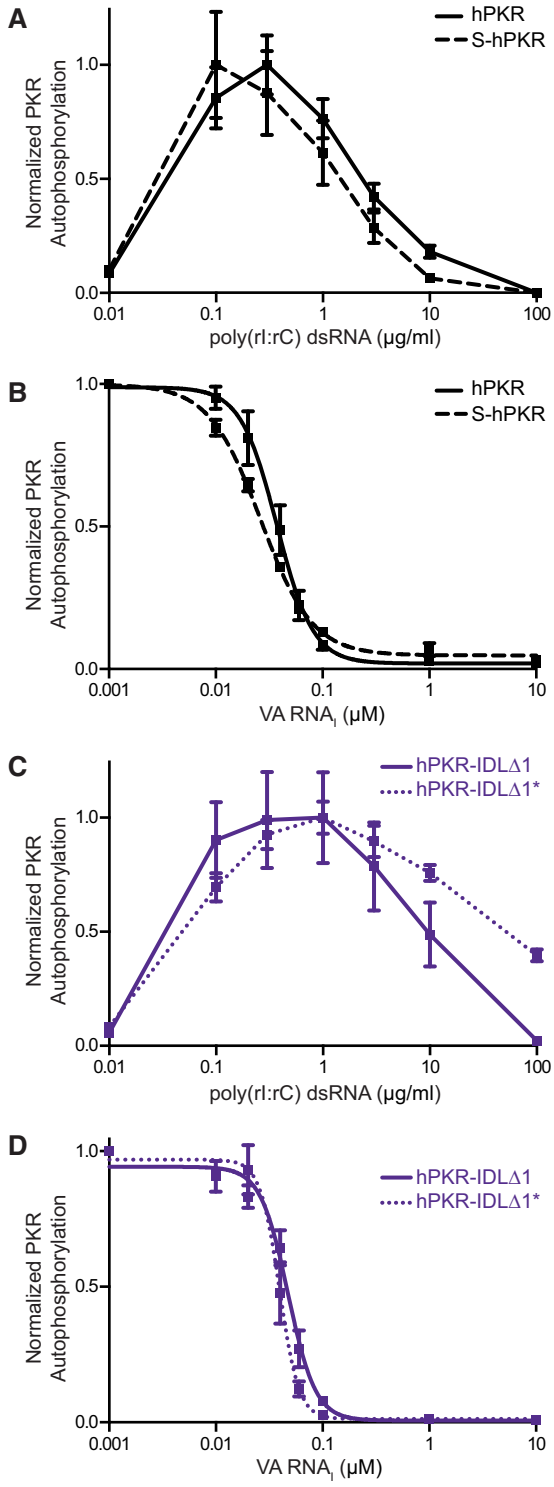

FIGURE 2. **Regulation of human PKR by dsRNA is unaffected by an N-terminal SUMO fusion or kinase domain loop deletion (ΔD338-N350).** *A*, comparison of poly(rI:rC) dsRNA-induced PKR autophosphorylation (activation) using human protein without (*hPKR*) and with (*S-hPKR*) an N-terminal SUMO domain. Activation follows the established bell-shaped response to poly(rI:rC) dsRNA concentration. *B*, as *panel A* but for adenovirus VA RNA$_I$-mediated inhibition of PKR autophosphorylation in the presence of a fixed concentration of poly(rI:rC) dsRNA activator. *C* and *D*, as *panels A* and *B*, but for comparison of hPKR with (*hPKR-IDLΔ1**) and without (*hPKR-IDLΔ1*) the KD deletion (ΔD338-N350) in addition to the IDLΔ1 deletion (ΔT197-T212) present in both proteins. Data in *panels B* and *D* were fit to determine the IC$_{50}$ values shown in Table 1.

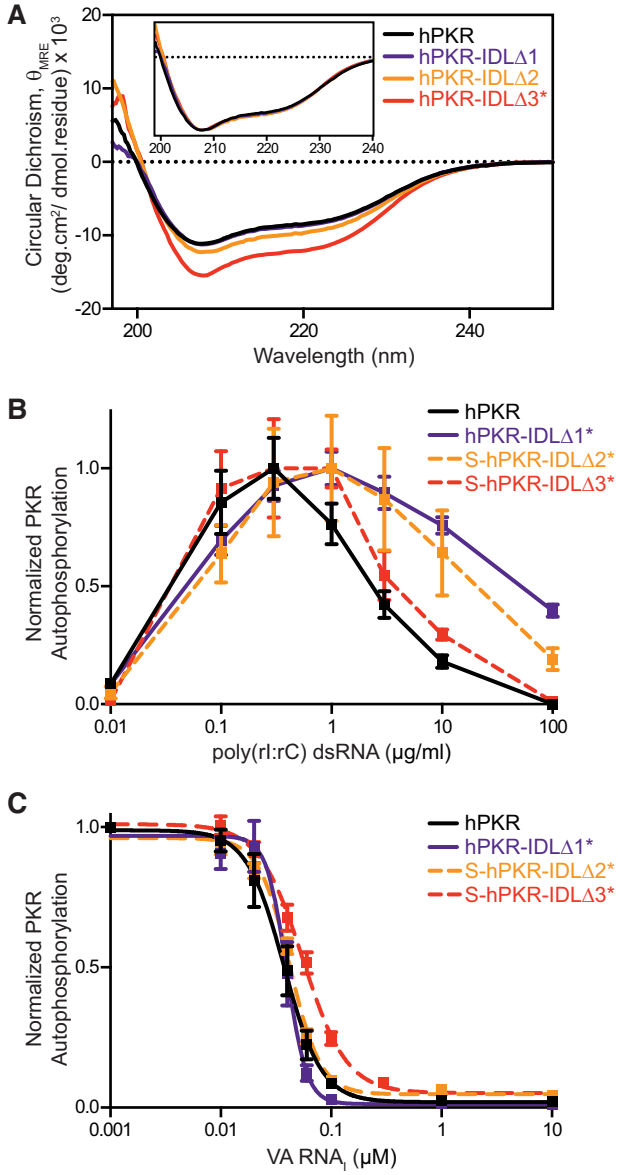

FIGURE 3. **The IDL of human PKR plays no role in its regulation by RNA.** *A*, CD spectra of hPKR (*black*), hPKR-IDLΔ1 (*purple*), hPKR-IDLΔ2 (*orange*), and hPKR-IDLΔ3* (*red*) demonstrate that PKR secondary structure is essentially unchanged upon deletion of the IDL. *Inset* shows the same spectra normalized to the minimum in CD signal at ~207 nm. *B*, comparison of poly(rI:rC) dsRNA-induced PKR autophosphorylation (activation) of hPKR, hPKR-IDLΔ1*, S-hPKR-IDLΔ2*, and S-hPKR-IDL3*. Color coding is the same as in *panel A*; *dashed lines* are used for proteins with an N-terminal SUMO tag, and *solid lines* indicate where the SUMO tag was cleaved or not included in the expression construct. *C*, as in *panel B* but for adenovirus VA RNA$_I$-mediated inhibition of PKR autophosphorylation in the presence of a fixed concentration of poly(rI:rC) dsRNA activator. Data were fit to determine the IC$_{50}$ values shown in Table 1.

as an N-terminal SUMO fusion: S-r/hPKR and S-h/rPKR, where r/h and h/r denote rat-NTD/human-CTD and human-NTD/rat-CTD PKRs, respectively (Fig. 1*C*).

As an initial test of the folding of each chimeric protein, we performed limited proteolysis using trypsin, as this approach is a useful tool for defining protein domain boundaries and has been applied to PKR previously (39). Furthermore, sequence conservation and *in silico* analysis of potential trypsin cleavage sites suggested that trypsin-sensitive regions might be com-

TABLE 1
Inhibition (IC_{50}) values for wild-type human, IDL deletion, and chimeric PKR proteins

Protein construct	PKR inhibition, IC_{50}	
	VA RNA_I	HIV-1 TAR
	nM	
hPKR	37 ± 6.3	ND
hPKR-IDLΔ1	47 ± 4.5	ND
hPKR-IDLΔ1*	39 ± 4.2	ND
S-hPKR-IDLΔ2*	42 ± 2.6	ND
S-hPKR-IDLΔ3*	55 ± 4.7	ND
S-hPKR	26 ± 2.1	139 ± 40
S-rPKR	175 ± 40	44,000 ± 2,900
S-h/rPKR	69 ± 6.7	1,300 ± 510
S-r/hPKR	48 ± 6.0	1,400 ± 340

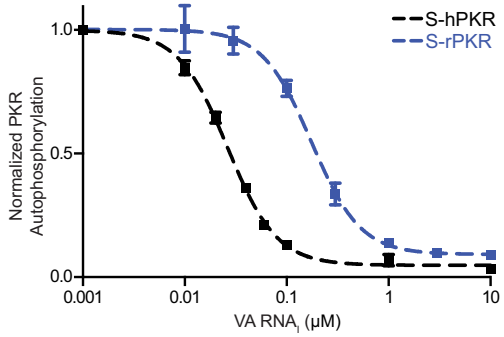

FIGURE 4. **Human Ad2 VA RNA_I is a poorer inhibitor of rat than human PKR.** Comparison of adenovirus VA RNA_I-mediated inhibition of PKR autophosphorylation in the presence of a fixed concentration of poly(rI:rC) dsRNA activator for S-hPKR and S-rPKR. Data were fit to determine the IC_{50} values shown in Table 1.

mon, if not precisely conserved, among hPKR, rPKR, and the chimeric proteins. Trypsin cleavage of untagged hPKR largely recapitulated the prior analysis with two major cleavage sites observed within the IDL and the C-terminal kinase domain (sites A and B, respectively; Fig. 5, *A* and *B*, *red* and *orange arrowheads*). An equivalent pattern of proteolytic fragments was observed for S-hPKR with two identical bands corresponding to one fragment each from sites A and B, with the former site also producing a larger N-terminal fragment (~43 kDa) due to the inclusion of the SUMO tag (Fig. 5, *A* and *B*). Additionally, with the increased size of the protein N terminus, a weak band (~23 kDa) was observed that corresponds to the previously noted third, minor cleavage site (site C; Fig. 5, *A* and *B*, *black arrowhead*).

S-rPKR showed a similar pattern of sensitivity to trypsin with a major cleavage site (denoted A′, *red open arrowheads*) corresponding to the main hPKR site A and a weaker site corresponding to hPKR site C between the two dsRBMs (denoted C′, *black open arrowhead*). Critically, both chimeric S-h/rPKR and S-r/hPKR proteins maintained this pattern of sensitivity to trypsin with major bands arising from cleavage at site A′ and a weaker band from site C′ (Fig. 5, *A* and *B*). We conclude from these analyses that the folded domains within each PKR construct are maintained and each protein possesses similar accessible unstructured regions within its truncated IDL and between the two dsRBMs.

We next tested the activation of S-rPKR and the two chimeric proteins by poly(rI:rC) dsRNA using a slot-blot assay and found a similar profile of autophosphorylation for each protein (Fig. 5*C*). Compared with S-hPKR, the response curves for the other proteins were shifted slightly to higher RNA activator concentration with the most pronounced effect observed for S-rPKR and S-h/rPKR, but critically, each followed the typical bell-shaped curve in response to increasing RNA concentration.

Although the correlation between autophosphorylation and downstream kinase activity on eIF2α substrate is established for hPKR, we used a second assay to directly measure the activity of rPKR and each chimeric protein on eIF2α in the absence or presence of a single concentration of poly(rI:rC) dsRNA (0.3 μg/ml). As expected, hPKR/S-hPKR showed both autophosphorylation and robust phosphorylation of eIF2α only in the presence of dsRNA, with no detectable activity in its absence (Fig. 5*D*, *left panel*). Although S-rPKR and each chimeric protein also showed strong up-regulation of autophosphorylation and eIF2α phosphorylation in the presence of dsRNA, S-rPKR and S-r/hPKR appeared to exhibit significant kinase activity even in the absence of the activator. To determine whether this activity might be an intrinsic property of these proteins and not an artifact of the expression or purification process, we first performed analytical gel filtration chromatography with purified PKR proteins. Both SUMO-tagged proteins (S-rPKR and S-r/hPKR) as well as the SUMO protease-treated r/hPKR, eluted exclusively at a volume corresponding to the monomeric protein (Fig. 5*E*). Although each protein was co-expressed with λ-protein phosphatase, to eliminate the possibility that the apparent constitutive activity of these proteins was due to uncontrolled phosphorylation and activation during expression in *E. coli*, the kinase assay was repeated after *in vitro* λ-protein phosphatase treatment. Again, although up-regulated by dsRNA, both S-rPKR and S-r/hPKR showed auto- and eIF2α phosphorylation activities in the absence of dsRNA (Fig. 5*D*, *right panel*). These activities were maintained in the cleaved form of the chimera, r/hPKR, indicating that the SUMO tag did not alter the protein activity. Thus, rPKR and the chimeric protein with the rat NTD appeared to possess low level, RNA-independent activity in a manner dependent upon the remaining IDL sequence and/or the N-terminal dsRBD (see "Discussion").

In summary, the data of Fig. 5 collectively demonstrate that the two chimeric human/rat domain swap PKR proteins retain the essential structural and functional properties of the parent proteins. Each has essentially identical domain folding and boundaries and exhibits both a similar response to dsRNA activator and capacity to phosphorylate eIF2 (albeit with some constitutive, dsRNA-independent activity for r/hPKR).

Both the Regulatory and Catalytic Domains of PKR Determine the Sensitivity to Inhibition by Human Virus Non-coding RNAs—As described above, human Ad2 VA RNA_I was a significantly weaker inhibitor of S-rPKR than the human homolog. We next tested the ability of this RNA to inhibit the two chimeric proteins and found, remarkably, that each was inhibited to a similar degree and between the two extremes of the human and rat proteins (Fig. 6*A* and Table 1). To establish that this effect is not specific to VA RNA_I, we tested the inhibitory activity of a second human viral non-coding RNA, HIV-1 TAR, against all four proteins. HIV-1 TAR acts as an inhibitor in its monomeric form but can activate PKR as an RNA dimer (35). Therefore,

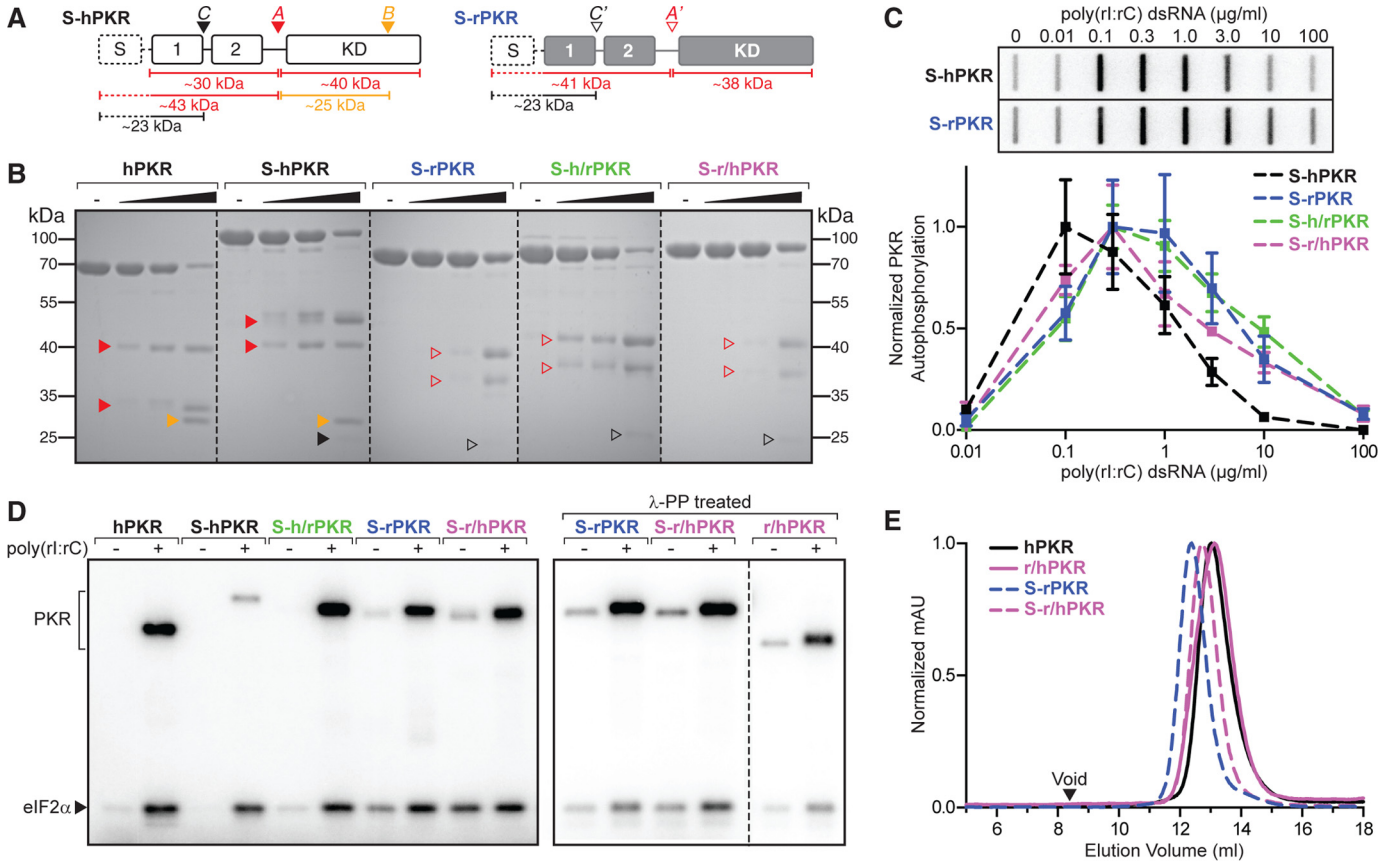

FIGURE 5. **Human, rat, and chimeric PKR proteins have conserved domain structure and responses to dsRNA activation.** *A*, established sites of cleavage in hPKR (*top*, *A–C*; *solid arrowheads*) (39) and equivalent sites (*A′* and *C′*; *open arrowheads*) in rPKR suggested by limited tryptic proteolysis. Approximate fragment sizes (with or without N-terminal SUMO) expected to be resolved by SDS-PAGE analysis are indicated *below each domain structure schematic*. *B*, SDS-PAGE analysis of limited tryptic proteolysis experiments for hPKR, S-hPKR, S-rPKR, S-h/rPKR, and S-r/hPKR. *Colored arrows* on the gels indicate positions of fragments shown in *panel A*. Increasing enzyme concentration over three consecutive lanes for each protein is indicated by the *triangle above the gel*; − denotes no trypsin treatment; kDa, protein standards of the molecular weight indicated on the *left* and *right sides* of the gel image. *C*, comparison of poly(rI:rC) dsRNA-induced PKR autophosphorylation (activation) of S-hPKR, S-rPKR, S-h/rPKR, and S-r/hPKR. Individual representative blots are shown for S-hPKR and S-rPKR (*top*). *D*, *left*, SDS-PAGE analysis of PKR autophosphorylation and PKR-mediated eIF2α phosphorylation in the absence or presence of a fixed concentration of poly(rI:rC) dsRNA (0.3 μg/ml) for hPKR, rPKR, and each chimeric protein. *Right*, gel image of equivalent analyses but after *in vitro* treatment with λ-protein phosphatase (λ-*PP*) for PKR proteins with apparent dsRNA-independent activation (presence of PKR and eIF2α phosphorylation in − *lane* in *left gel image*). *E*, gel filtration analysis of purified proteins treated with λ-protein phosphatase in *panel D* compared with hPKR. *mAU*, milliabsorbance units.

before performing kinase inhibition assays we confirmed that our HIV-1 TAR RNA preparation was exclusively monomeric (Fig. 6*B*, *inset*). We found that HIV-1 TAR RNA was a dramatically poorer inhibitor of S-rPKR compared with S-hPKR, with a substantially greater differential activity than observed with VA RNA_I (7- and >300-fold differences in IC_{50} for VA RNA_I and TAR RNA, respectively; Fig. 6*B* and Table 1). Furthermore, each chimeric protein again possessed a similar inhibitory activity falling between the two extremes of S-hPKR and S-rPKR.

Finally, to examine whether differences in PKR-RNA binding affinity underpin the observed differences in inhibition, we used isothermal titration calorimetry to measure S-hPKR and S-rPKR binding affinity for VA RNA_I and HIV-1 TAR RNA. Remarkably, essentially the same binding affinity was determined for each protein with both non-coding RNAs, with all K_d values in the range 210–275 nM (Fig. 6, *C* and *D*). Curiously, however, the K_d for S-hPKR/VA RNA_I interaction was ~5-fold weaker than we previously measured for hPKR with the same RNA (32). Although performed under otherwise similar solution conditions, this difference in affinity had two obvious potential origins: the presence of the N-terminal SUMO tag or the reversal of the titrant and titrand in the current experiments (necessary due to the lower maximum concentration that we were able to achieve for S-rPKR). We, therefore, performed additional titrations with hPKR and VA RNA_I to examine the effect of titration order (*i.e.* hPKR titrated into VA RNA_I, compared with VA RNA_I titrated into hPKR) using common buffer solutions and preparations of each component. Strikingly, a K_d of 290 nM was obtained with hPKR in the cell but reverting to the previously used configuration (*i.e.* protein in the syringe) resulted in a K_d of 50 nM comparable to the published value for hPKR (32). Thus, the titration orientation, and not the presence of the N-terminal SUMO tag, is the origin of the modestly weaker PKR-RNA affinities determined here.

In conclusion, we find that viral non-coding RNA inhibition of hPKR is dependent on features of both the N-terminal dsRNA binding regulatory domain and the C-terminal kinase domain but essentially independent of the binding affinity of the protein-RNA complex.

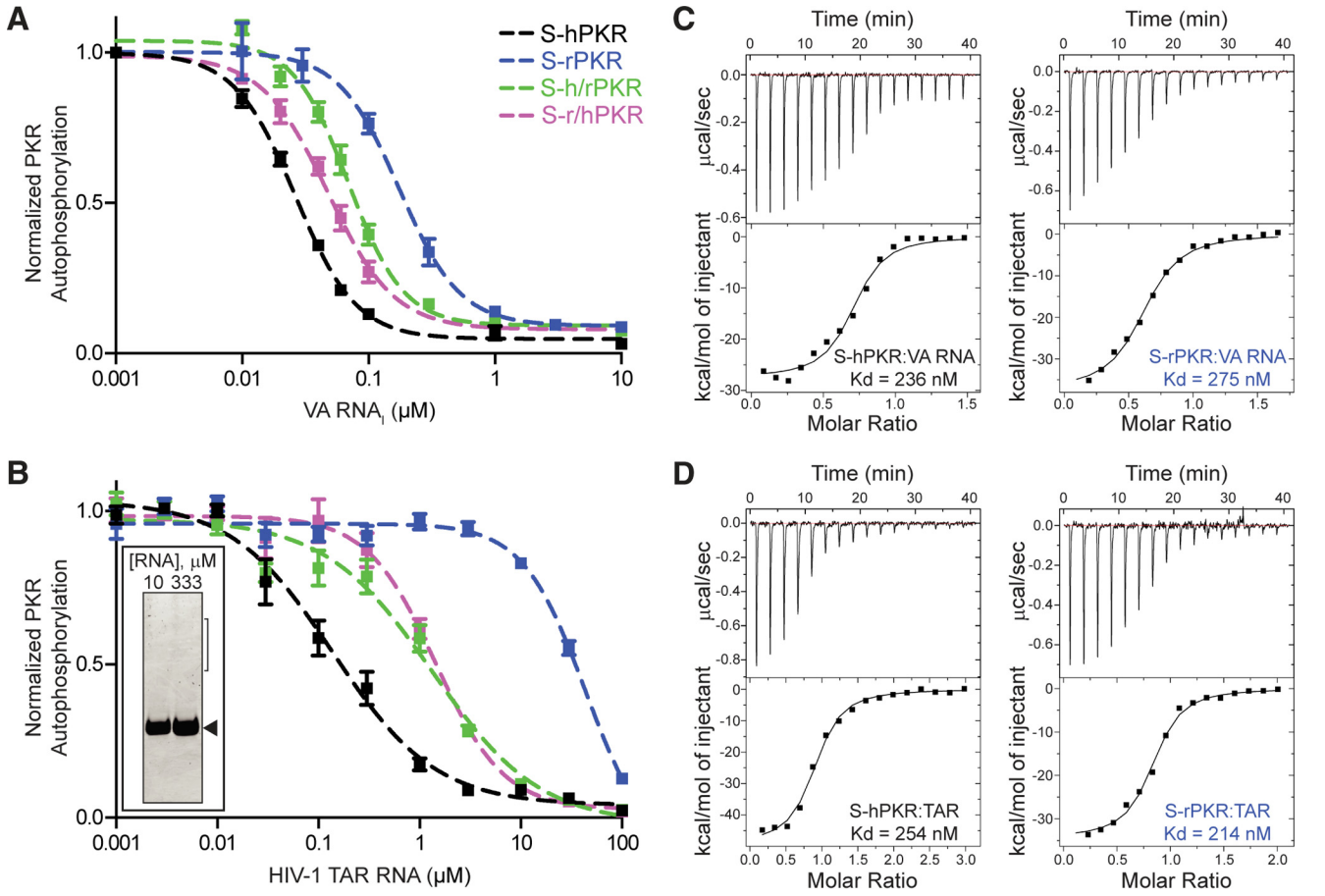

FIGURE 6. **Both domains of hPKR contribute to inhibition by viral non-coding RNAs.** *A*, comparison of adenovirus VA RNA$_I$-mediated inhibition of PKR autophosphorylation in the presence of a fixed concentration of poly(rI:rC) dsRNA activator for S-hPKR, S-rPKR, and each domain swap chimera (S-hPKR and S-rPKR data are the same as those in Fig. 4). *B*, as in *panel A*, but for inhibition by HIV-1 TAR RNA. Color coding is the same in *panels A* and *B*, and data in each were fit to determine the IC_{50} values shown in Table 1. *Inset*, native gel analysis demonstrating the monomeric nature (*arrowhead*) of the HIV-1 TAR RNA preparation; PKR-activating dimeric species would be expected in the region of the gel marked by a *vertical bracket*. Example isothermal titration calorimetry analyses are shown for S-hPKR (*left*) and S-rPKR (*right*) interaction with VA RNA$_I$ (*C*) and HIV-1 TAR (*D*) RNA.

Discussion

The modular architecture of multidomain proteins can confer benefits such as adding cooperative functions (40), and the regions linking them (the IDLs) can couple the activities of regulatory and catalytic domains (41, 42). Additionally, alterations in the length of these IDL "hinge" regions have been shown to impact protein stability, folding rates, and domain-domain orientation in functionally diverse proteins, such as Src family kinases, polyketide synthase, and myosin (41, 43, 44). In the current work, our goal was to assess the contributions of the IDL and folded domains of the human eIF2 kinase PKR to its regulation by RNA.

The hPKR IDL has been proposed to mediate dynamic communication between its N-terminal regulatory dsRBD and C-terminal KD during activation by dsRNA as well as potentially play a role in PKR self-association and activity (4, 6, 14). To directly define the role of hPKR IDL in regulation of the kinase activity by RNA, we created three IDL deletion variants of hPKR guided by alignment of the human and rodent PKR sequences. Contrary to our initial expectation based upon the putative role(s) of the IDL, we found that deletion of the entire hPKR IDL had no effect on PKR activation by a synthetic dsRNA activator poly(rI:rC) or on its inhibition by the adenoviral non-coding transcript VA RNA$_I$. The hPKR IDL, therefore, appears to be entirely dispensable for RNA-mediated regulation and is not necessary to relay an RNA binding signal from the N-terminal regulatory domain to the C-terminal KD.

Although the IDL may not be necessary for PKR dimerization/activation or inhibition when these processes are driven by RNA binding *in vitro*, our results do not fully exclude a contribution to PKR function *in vivo*. Additionally, although our analyses show that an N-terminal SUMO fusion has no influence on RNA-mediated regulation of PKR, SUMOylation is proposed to modulate PKR antiviral activity when appended to specific lysine residues, one of which is located in the NTD near its junction with the IDL (45). Fully excluding roles for the IDL in RNA-mediated regulation or the influence of adjacent post-translational modifications on PKR activity will thus require further extensive cell-based experiments.

The IDL may also play important roles in PKR function in other contexts. In addition to acting as a cytosolic dsRNA sensor in an antiviral capacity, hPKR is involved in other key cellular processes (46, 47) that may require the IDL to promote or block activity. For example, the IDL is serine- and threonine-rich and is a potential site of post-translational modification and, thus, regulation by other cellular kinases. Regions of the

IDL in addition to the folded domains are also targeted by viral PKR inhibitors (48), strongly implying the IDL either contributes to the control of PKR activity or may be manipulated for this purpose. Adoption of defined IDL structure and/or interactions at the PKR dimer interface may acquire functional relevance in RNA-independent activation or inhibition processes while being redundant in the context of RNA-mediated regulation.

Although the biological significance of RNA-independent hPKR self-association and activation at high protein concentrations is not clear, a role for the IDL in dimerization in the absence of RNA remains possible (4, 49). The PKR IDL varies considerably in length between species, with the longest sequence found in hPKR (~80 amino acid residues), compared with mouse/rat (~55–60 residues) and other rodents, *e.g.* Golden hamster (*M. auratus* PKR with ~20 residues). Thus, species-specific differences in the contribution of the IDL to PKR regulation are possible. We found that rPKR has detectable auto- and eIF2α phosphorylation activity in the absence of RNA at much lower protein concentrations than are required for hPKR. In further support of a role for the IDL in controlling such RNA-independent dimerization, we found that the Golden hamster (*M. auratus* PKR) variant 2 appears to be fully constitutively active and did not bind or respond to dsRNA activator despite conservation of key residues for RNA interaction within the NTD.[4] *M. auratus* PKR has a minimal IDL (Fig. 1*B*) containing only the conserved C-terminal segment proposed to promote self-association, possibly through a transition to an ordered structure in the context of the dimer interface (49).

Based on the data presented here, the contributions of the IDL and NTD to the greater propensity for RNA-independent activity in rPKR cannot be fully discerned. RNA-independent activity at the low PKR concentration used in our kinase assay was maintained in the rat NTD/human CTD domain swap but not the alternate chimeric protein. This activity might, therefore, depend on features of the rPKR NTD (common to rPKR and r/hPKR), differences in the IDL sequences between the human and rat proteins, or potentially both. Although each contains the most conserved C-terminal portion of the IDL, hPKR and rPKR differ significantly in their N-terminal IDL sequence and length, and r/hPKR lacks the N-terminal 24 residues of the hPKR IDL. An intriguing possibility is that sequences within the hPKR IDL, one or more absent in rPKR, may compete to hinder or promote PKR dimerization in the absence of RNA. Indeed, alanine substitution of either Ser-242 or Thr-255 at the C-terminal end of the IDL, residues which are unique to hPKR compared with the rodent proteins, has been shown to exacerbate the impact on kinase activity conferred by substitution of the conserved Thr-258 in the KD (50). However, a simple, direct competition between N-terminal and C-terminal sequences in the hPKR IDL would be expected to result in similar retention of constitutive activity in the alternate h/rPKR chimera (containing the majority of the rPKR IDL), which we did not observe. Therefore, the possibility remains that the rPKR NTD has the major influence on the variation of PKR self-association either directly or by altering the context of the IDL sequences involved. High resolution structures of intact PKR in the absence and presence of RNA will be required to fully reveal the molecular details of control of PKR activation via RNA-driven dimerization and PKR self-association.

Our analyses of the human/rat chimeric PKR proteins also revealed an unanticipated significance for the C-terminal KD in determining the sensitivity of PKR activity to human viral non-coding RNAs. Although we found that hPKR, rPKR, and both domain swap chimeric proteins responded similarly to dsRNA activator, rPKR was much more weakly inhibited by two human viral non-coding RNAs, and each chimeric protein had a similar intermediate sensitivity. We additionally confirmed that the observed difference in sensitivity between hPKR and rPKR is independent of the protein-RNA binding affinities. Host factors must continually adapt to evade pathogen-derived inhibitors and substrate mimics; PKR in particular has undergone recent episodes of intense evolutionary adaption that resulted in changes in both domains of primate PKR sequences, including multiple protein surfaces in the C-terminal KD that control interaction with eIF2 (51). Given the greater evolutionary distance between human and rat PKR, the latter protein's lower sensitivity to human viral RNAs is not unexpected. However, our finding suggests that human viral non-coding RNAs are also adapted to specifically exploit sequence or structural features of the hPKR C-terminal KD to confer their inhibitory effect.

Author Contributions—G. L. C. conceived and coordinated the study. S. S. and S. L. S. performed and analyzed the results of all the experiments. All authors reviewed the results, wrote the manuscript, and approved the final version.

Acknowledgments—We are grateful to our colleagues in the Conn laboratory and members of Dr. Christine Dunham's group for many useful discussions during this work and preparation of the manuscript. The Auto-iTC$_{200}$ instrument was purchased with support from the National Science Foundation Major Research Instrumentation Program (MRI) program (Grant 104177), the Winship Cancer Institute's shared resource program, and the Biochemistry Department of Emory University.

[4] S. L. Schwartz and G. L. Conn, unpublished information.

References

1. Donnelly, N., Gorman, A. M., Gupta, S., and Samali, A. (2013) The eIF2α kinases: their structures and functions. *Cell. Mol. Life Sci.* **70,** 3493–3511
2. Nanduri, S., Carpick, B. W., Yang, Y., Williams, B. R, and Qin, J. (1998) Structure of the double-stranded RNA-binding domain of the protein kinase PKR reveals the molecular basis of its dsRNA-mediated activation. *EMBO J.* **17,** 5458–5465
3. Dar, A. C., Dever, T. E., and Sicheri, F. (2005) Higher-order substrate recognition of eIF2α by the RNA-dependent protein kinase PKR. *Cell* **122,** 887–900
4. McKenna, S. A., Lindhout, D. A., Kim, I., Liu, C. W., Gelev, V. M., Wagner, G., and Puglisi, J. D. (2007) Molecular framework for the activation of RNA-dependent protein kinase. *J. Biol. Chem.* **282,** 11474–11486
5. Lemaire, P. A., Tessmer, I., Craig, R., Erie, D. A., and Cole, J. L. (2006) Unactivated PKR exists in an open conformation capable of binding nucleotides. *Biochemistry* **45,** 9074–9084
6. Wu, S., and Kaufman, R. J. (1997) A model for the double-stranded RNA (dsRNA)-dependent dimerization and activation of the dsRNA-activated protein kinase PKR. *J. Biol. Chem.* **272,** 1291–1296
7. Robertson, H. D., and Mathews, M. B. (1996) The regulation of the protein

kinase PKR by RNA. *Biochimie* **78,** 909–914
8. Cole, J. L. (2007) Activation of PKR: an open and shut case? *Trends Biochem. Sci.* **32,** 57–62
9. Langland, J. O., and Jacobs, B. L. (1992) Cytosolic double-stranded RNA-dependent protein kinase is likely a dimer of partially phosphorylated M_r = 66,000 subunits. *J. Biol. Chem.* **267,** 10729–10736
10. Lemaire, P. A., Lary, J., and Cole, J. L. (2005) Mechanism of PKR activation: dimerization and kinase activation in the absence of double-stranded RNA. *J. Mol. Biol.* **345,** 81–90
11. Gabel, F., Wang, D., Madern, D., Sadler, A., Dayie, K., Daryoush, M. Z., Schwahn, D., Zaccai, G., Lee, X., and Williams, B. R. (2006) Dynamic flexibility of double-stranded RNA activated PKR in solution. *J. Mol. Biol.* **359,** 610–623
12. Patel, R. C., Stanton, P., McMillan, N. M., Williams, B. R., and Sen, G. C. (1995) The interferon-inducible double-stranded RNA-activated protein kinase self-associates *in vitro* and *in vivo*. *Proc. Natl. Acad. Sci. U.S.A.* **92,** 8283–8287
13. Ung, T. L., Cao, C., Lu, J., Ozato, K., and Dever, T. E. (2001) Heterologous dimerization domains functionally substitute for the double-stranded RNA binding domains of the kinase PKR. *EMBO J.* **20,** 3728–3737
14. Vattem, K. M., Staschke, K. A., and Wek, R. C. (2001) Mechanism of activation of the double-stranded-RNA-dependent protein kinase, PKR: role of dimerization and cellular localization in the stimulation of PKR phosphorylation of eukaryotic initiation factor-2 (eIF2). *Eur. J. Biochem.* **268,** 3674–3684
15. Lee, K., Kunkeaw, N., Jeon, S. H., Lee, I., Johnson, B. H., Kang, G. Y., Bang, J. Y., Park, H. S., Leelayuwat, C., and Lee, Y. S. (2011) Precursor miR-886, a novel noncoding RNA repressed in cancer, associates with PKR and modulates its activity. *RNA* **17,** 1076–1089
16. Lee, Y. S. (2015) A novel type of non-coding RNA, nc886, implicated in tumor sensing and suppression. *Genomics Inform.* **13,** 26–30
17. Takeuchi, O., and Akira, S. (2010) Pattern recognition receptors and inflammation. *Cell* **140,** 805–820
18. Dey, M., Mann, B. R., Anshu, A., and Mannan, M. A. (2014) Activation of protein kinase PKR requires dimerization-induced cis-phosphorylation within the activation loop. *J. Biol. Chem.* **289,** 5747–5757
19. Dauber, B., and Wolff, T. (2009) Activation of the antiviral kinase PKR and viral countermeasures. *Viruses* **1,** 523–544
20. Ma, Y., and Mathews, M. B. (1996) Structure, function, and evolution of adenovirus-associated RNA: a phylogenetic approach. *J. Virol.* **70,** 5083–5099
21. Mathews, M. B., and Shenk, T. (1991) Adenovirus virus-associated RNA and translation control. *J. Virol.* **65,** 5657–5662
22. Vachon, V. K., and Conn, G. L. (2015) Adenovirus VA RNA: an essential pro-viral non-coding RNA. *Virus Res.* 10.1016/j.virusres.2015.06.018
23. Clarke, P. A., Schwemmle, M., Schickinger, J., Hilse, K., and Clemens, M. J. (1991) Binding of Epstein Barr Virus small RNA EBER-1 to the double stranded RNA-activated protein kinase DAI. *Nucleic Acids Res.* **19,** 243–248
24. Sharp, T. V., Schwemmle, M., Jeffrey, I., Laing, K., Mellor, H., Proud, C. G., Hilse, K., and Clemens, M. J. (1993) Comparative analysis of the regulation of the interferon-inducible protein kinase PKR by Epstein Barr virus RNAs EBER-1 and EBER-2 and Adenovirus VA(I) RNA. *Nucleic Acids Res.* **21,** 4483–4490
25. Roy, S., Agy, M., Hovanessian, A. G., Sonenberg, N., and Katze, M. G. (1991) The integrity of the stem structure of human immunodeficiency virus type 1 Tat-responsive sequence of RNA is required for interaction with the interferon-induced 68,000-Mr protein kinase. *J. Virol.* **65,** 632–640
26. Launer-Felty, K., Wong, C. J., and Cole, J. L. (2015) Structural analysis of adenovirus VAI RNA defines the mechanism of inhibition of PKR. *Biophys. J.* **108,** 748–757
27. Miyazaki, K. (2011) MEGAWHOP cloning: a method of creating random mutagenesis libraries via megaprimer PCR of whole plasmids. *Methods Enzymol.* **498,** 399–406
28. Miyazaki, K., and Takenouchi, M. (2002) Creating random mutagenesis libraries using megaprimer PCR of whole plasmid. *Biotechniques* **33,** 1033–1034
29. Studier, F. W. (2005) Protein production by auto-induction in high-density shaking cultures. *Protein Expr. Purif.* **41,** 207–234
30. Wahid, A. M., Coventry, V. K., and Conn, G. L. (2008) Systematic deletion of the adenovirus-associated RNAI terminal stem reveals a surprisingly active RNA inhibitor of double-stranded RNA-activated protein kinase. *J. Biol. Chem.* **283,** 17485–17493
31. Pe'ery, T., and Mathews, M. B. (1997) Synthesis and purification of single-stranded RNA for use in experiments with PKR and in cell-free translation systems. *Methods* **11,** 371–381
32. Wilson, J. L., Vachon, V. K., Sunita, S., Schwartz, S. L., and Conn, G. L. (2014) Dissection of the adenoviral VA RNAI central domain structure reveals minimum requirements for RNA-mediated inhibition of PKR. *J. Biol. Chem.* **289,** 23233–23245
33. Gurevich, V. V. (1996) Use of bacteriophage RNA polymerase in RNA synthesis. *Methods Enzymol.* **275,** 382–397
34. Linpinsel, J. L., and Conn, G. L. (2012) General protocols for preparation of plasmid DNA template, RNA *in vitro* transcription, and RNA purification by denaturing PAGE. *Methods Mol. Biol.* **941,** 43–58
35. Heinicke, L. A., Wong, C. J., Lary, J., Nallagatla, S. R., Diegelman-Parente, A., Zheng, X., Cole, J. L., and Bevilacqua, P. C. (2009) RNA dimerization promotes PKR dimerization and activation. *J. Mol. Biol.* **390,** 319–338
36. Greenfield, N. J. (1996) Methods to estimate the conformation of proteins and polypeptides from circular dichroism data. *Anal. Biochem.* **235,** 1–10
37. Hunter, T., Hunt, T., Jackson, R. J., and Robertson, H. D. (1975) Characteristics of inhibition of protein synthesis by double-stranded ribonucleic acid in reticulocyte lysates. *J. Biol. Chem.* **250,** 409–417
38. Kostura, M., and Mathews, M. B. (1989) Purification and activation of the double-stranded RNA-dependent eIF-2 kinase DAI. *Mol. Cell. Biol.* **9,** 1576–1586
39. Anderson, E., and Cole, J. L. (2008) Domain stabilities in protein kinase R (PKR): evidence for weak interdomain interactions. *Biochemistry* **47,** 4887–4897
40. George, R. A., and Heringa, J. (2002) An analysis of protein domain linkers: their classification and role in protein folding. *Protein Eng.* **15,** 871–879
41. Briggs, S. D., and Smithgall, T. E. (1999) SH2-kinase linker mutations release Hck tyrosine kinase and transforming activities in Rat-2 fibroblasts. *J. Biol. Chem.* **274,** 26579–26583
42. LaFevre-Bernt, M., Sicheri, F., Pico, A., Porter, M., Kuriyan, J., and Miller, W. T. (1998) Intramolecular regulatory interactions in the Src family kinase Hck probed by mutagenesis of a conserved tryptophan residue. *J. Biol. Chem.* **273,** 32129–32134
43. Gokhale, R. S., Tsuji, S. Y., Cane, D. E., and Khosla, C. (1999) Dissecting and exploiting intermodular communication in polyketide synthases. *Science* **284,** 482–485
44. Ikebe, M., Kambara, T., Stafford, W. F., Sata, M., Katayama, E., and Ikebe, R. (1998) A hinge at the central helix of the regulatory light chain of myosin is critical for phosphorylation-dependent regulation of smooth muscle myosin motor activity. *J. Biol. Chem.* **273,** 17702–17707
45. de la Cruz-Herrera, C. F., Campagna, M., García, M. A., Marcos-Villar, L., Lang, V., Baz-Martínez, M., Gutiérrez, S., Vidal, A., Rodríguez, M. S., Esteban, M., and Rivas, C. (2014) Activation of the double-stranded RNA-dependent protein kinase PKR by small ubiquitin-like modifier (SUMO). *J. Biol. Chem.* **289,** 26357–26367
46. García, M. A., Meurs, E. F., and Esteban, M. (2007) The dsRNA protein kinase PKR: virus and cell control. *Biochimie* **89,** 799–811
47. Williams, B. R. (1999) PKR; a sentinel kinase for cellular stress. *Oncogene* **18,** 6112–6120
48. Langland, J. O., Cameron, J. M., Heck, M. C., Jancovich, J. K., and Jacobs, B. L. (2006) Inhibition of PKR by RNA and DNA viruses. *Virus Res.* **119,** 100–110
49. VanOudenhove, J., Anderson, E., Krueger, S., and Cole, J. L. (2009) Analysis of PKR structure by small-angle scattering. *J. Mol. Biol.* **387,** 910–920
50. Taylor, D. R., Lee, S. B., Romano, P. R., Marshak, D. R., Hinnebusch, A. G., Esteban, M., and Mathews, M. B. (1996) Autophosphorylation sites participate in the activation of the double-stranded-RNA-activated protein kinase PKR. *Mol. Cell. Biol.* **16,** 6295–6302
51. Elde, N. C., Child, S. J., Geballe, A. P., and Malik, H. S. (2009) Protein kinase R reveals an evolutionary model for defeating viral mimicry. *Nature* **457,** 485–489